iScience

CellPress
OPEN ACCESS

Article

An innovative index for separating the effects of temperature and precipitation on global vegetation change

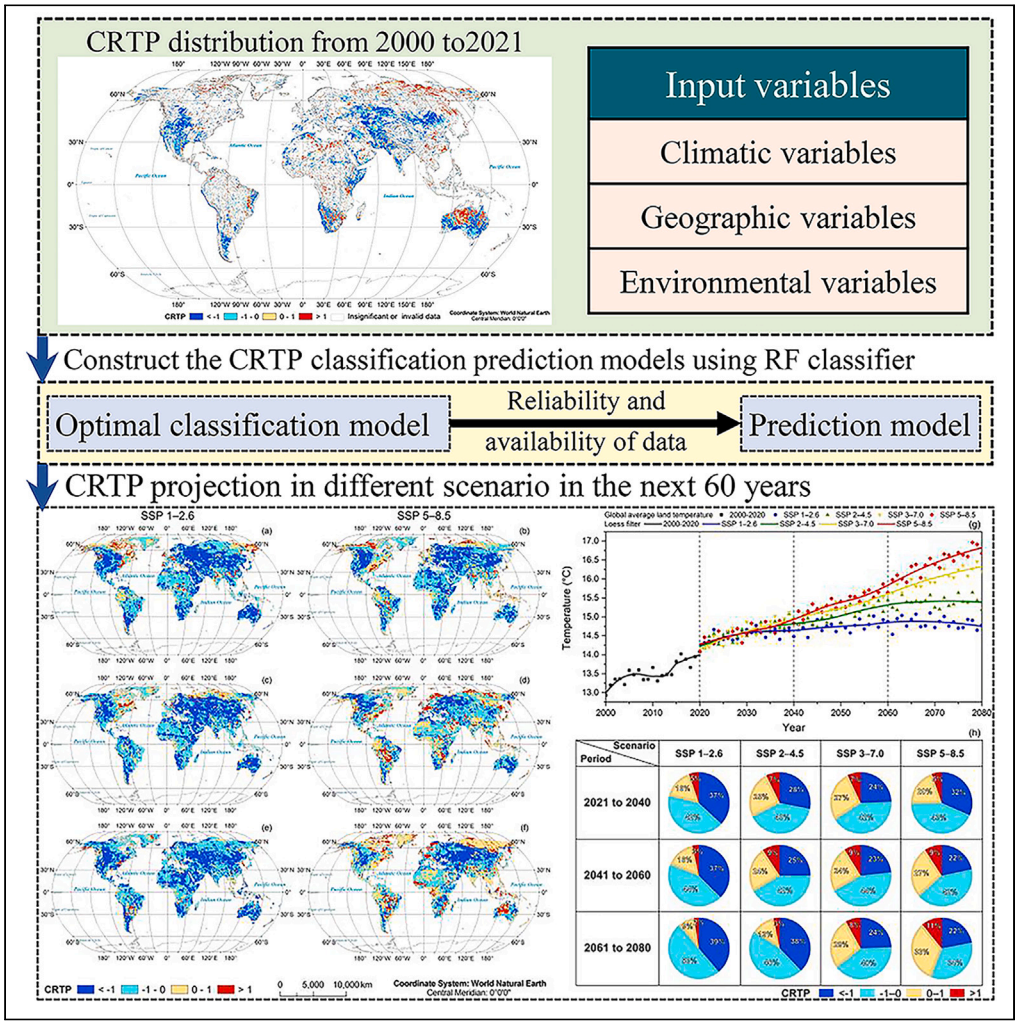

Xueqin Zhang, Xiang Li

zhangxq@igsnrr.ac.cn

Highlights

Index CRTP separates the impacts of two key climatic factors on vegetation change

Precipitation dominates over 70% of the significant global vegetation change

Latitude and longitude regulate the distribution pattern of different CRTP types

Temperature impacts on vegetation will enhance under higher radiative forcings

Zhang & Li, iScience 26, 106972
June 16, 2023
https://doi.org/10.1016/j.isci.2023.106972

iScience

CellPress
OPEN ACCESS

Article

An innovative index for separating the effects of temperature and precipitation on global vegetation change

Xueqin Zhang[1,3,*] and Xiang Li[1,2]

SUMMARY

Temperature and precipitation changes are among the vital climatic driving forces of global vegetation change. However, the strategy to separate the relative contributions of these two critical climatic factors is still lacking. Here, we propose an index CRTP (contribution ratio of temperature and precipitation) to quantify their impacts on vegetation and then construct the CRTP classification prediction models based on climatic, geographic, and environmental factors using the Random Forest classifier. We find that precipitation predominates more than 70% of the significant vegetation change, mainly located in the low and middle latitudes during 2000–2021. Precipitation will remain the dominant climatic factor affecting global vegetation change in the coming six decades, whereas areas with temperature-dominated vegetation change will expand under higher radiative forcings. Hopefully, the promising index CRTP will be applied in the research about climatic attribution for regional vegetation degradation, monitoring drought-type conversion, and alarming the potential ecological risk.

INTRODUCTION

Terrestrial ecosystems and climate systems interact and are closely coupled.[1,2] Global warming profoundly impacts the global terrestrial ecosystem, specifically vegetation change. Most global vegetated regions are greening, dominated by climate change and CO_2 fertilization effects.[3] Warming temperature increases the biomass across all the terrestrial plants,[4] lengthens the green cover season,[5] and reshapes the global biodiversity.[6] Meanwhile, climate related vegetation change has many negative consequences for both the natural environment and human society,[7] such as increasing wildfire hazards,[8] raising the likelihood of seasonal allergies,[9] dieback of the rainforest,[10] and decoupling species interactions.[11] Therefore, how vegetation responds to climate change is paramount to explicitly disclose the relationship between climate and vegetation at global and regional scales.

Temperature and precipitation can accurately describe the hydrothermal conditions affecting vegetation growth, so they are commonly considered essential climatic factors influencing global vegetation change.[12,13] Temperature change is usually responsible for the regional ensemble vegetation change,[14] whereas the difference in precipitation explains most of the annual variation in spatial patterns.[15] Meanwhile, the supremacy of temperature and precipitation on vegetation change is interchanged with regions, seasons, and vegetation species.[16] The temperature dominates the vegetation change in the northern middle to high latitudes or high altitudes,[12,17] yet precipitation is the critical climatic factor impacting vegetation in southern semiarid regions.[12,18] The vegetation's sensitivity to temperature and precipitation in summer is higher than in other seasons.[19] In addition, precipitation may become grasslands' primary vegetation growth-limiting factor, especially in the growing season; the mean temperature is the dominant growth-limiting factor for forest[16] and alpine vegetation.[20]

Despite the research improvements mentioned above, the quantitative strategy to separate the relative contributions of temperature and precipitation, or whether temperature or precipitation dominates vegetation change in a specific region, is still lacking. Research on the dominant climatic factor affecting vegetation change is indispensable for ecosystem management.[21,22] Projected temperature and precipitation change will have potentially negative consequences for the ecosystem, such as increasing wildfire[23] and decreasing biodiversity.[6] In turn, vegetation responses to climate change are complex and chaotic,[24]

[1]Key Lab of Land Surface Pattern and Simulation, Institute of Geographic Sciences and Natural Resources Research, 11A, Datun Road, Beijing 100101, China

[2]University of Chinese Academy of Sciences, No. 19A, Yuquan Road, Beijing 100049, China

[3]Lead contact

*Correspondence: zhangxq@igsnrr.ac.cn

https://doi.org/10.1016/j.isci.2023.106972

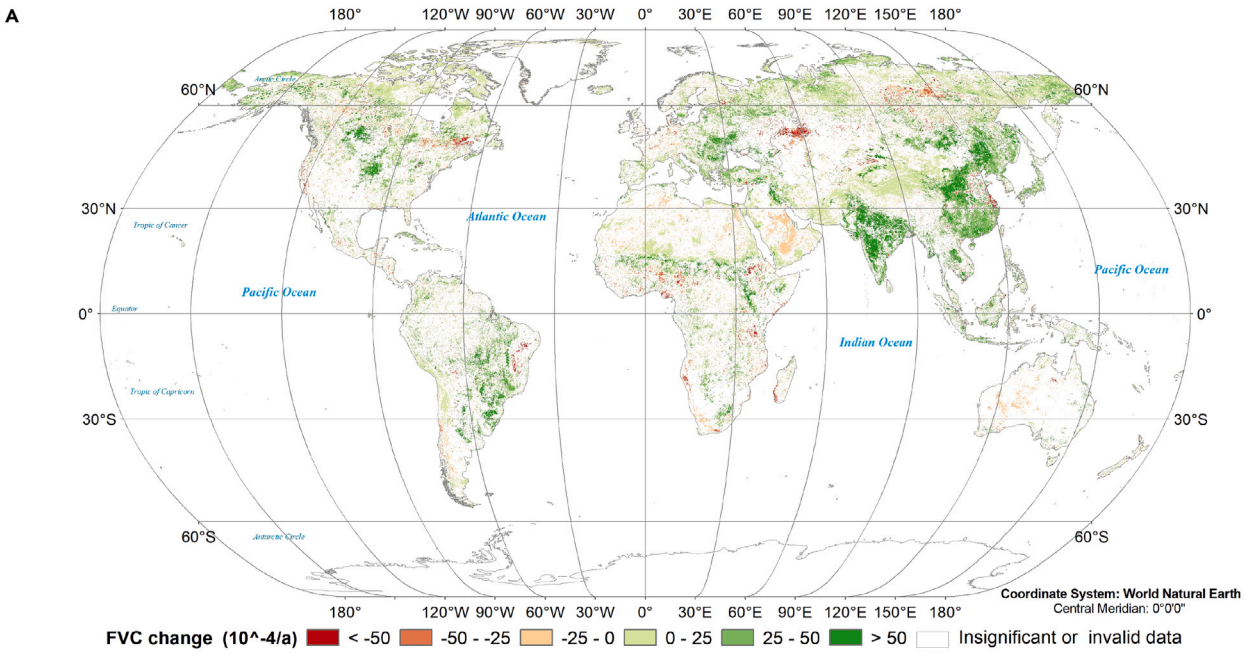
A
180° 120°W 90°W 60°W 30°W 0° 30°E 60°E 90°E 120°E 150°E 180°
60°N
30°N
0°
30°S
60°S
Arctic Circle
Tropic of Cancer
Equator
Tropic of Capricorn
Antarctic Circle
Atlantic Ocean
Pacific Ocean
Indian Ocean
Pacific Ocean
Coordinate System: World Natural Earth
Central Meridian: 0°0'0"
FVC change (10^-4/a) < -50 -50 - -25 -25 - 0 0 - 25 25 - 50 > 50 Insignificant or invalid data

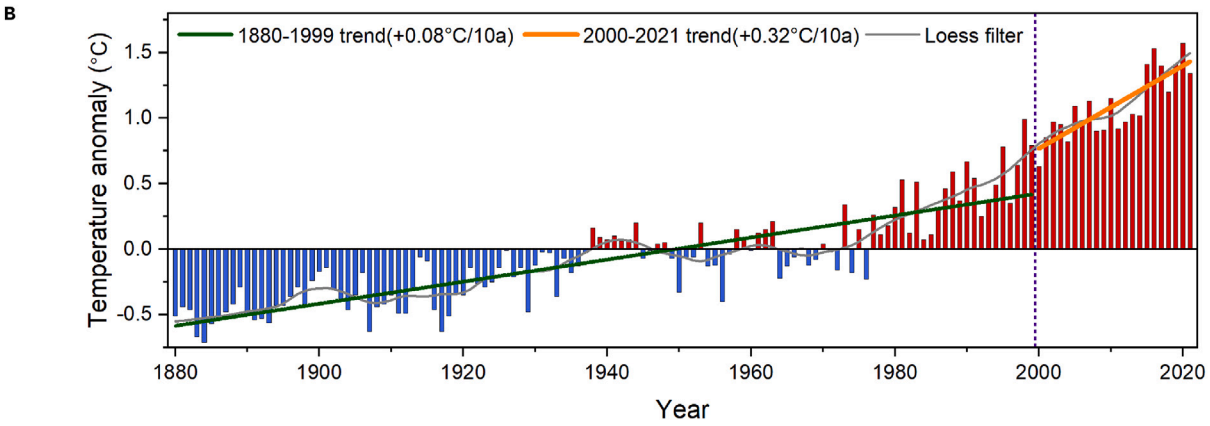
B
1880-1999 trend(+0.08°C/10a)
2000-2021 trend(+0.32°C/10a)
Loess filter
Temperature anomaly (°C)
1.5
1.0
0.5
0.0
-0.5
1880
1900
1920
1940
1960
1980
2000
2020
Year

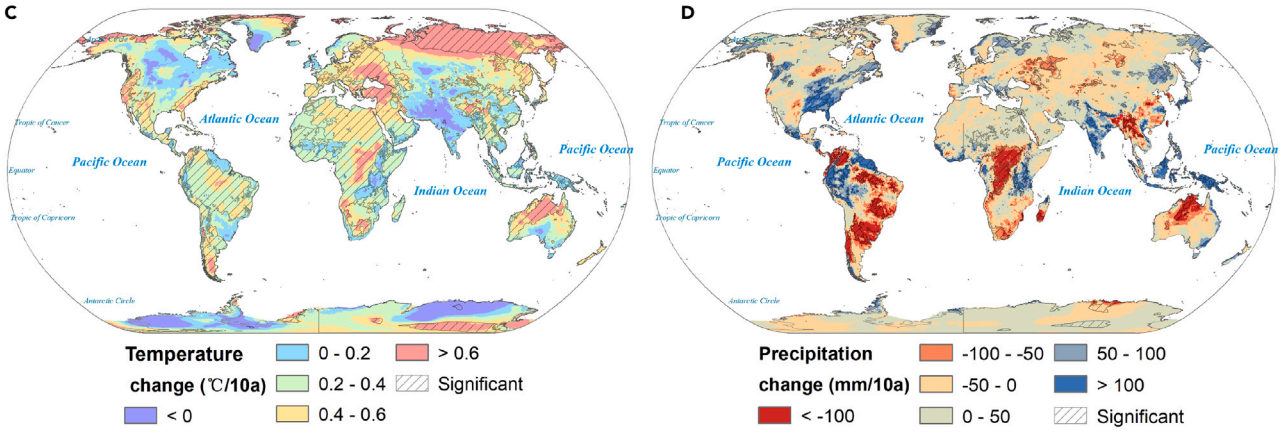
C
Atlantic Ocean
Pacific Ocean
Indian Ocean
Pacific Ocean
Temperature change (℃/10a)
< 0
0 - 0.2
0.2 - 0.4
0.4 - 0.6
> 0.6
Significant
D
Atlantic Ocean
Pacific Ocean
Indian Ocean
Pacific Ocean
Precipitation change (mm/10a)
< -100
-100 - -50
-50 - 0
0 - 50
50 - 100
> 100
Significant

Figure 1. Global vegetation and climate change

Global vegetation and climate change, including the distribution of global vegetation change from 2000 to 2021 (A), global temperature changes from 1880 to 2021 (B), and the distribution of global temperature and precipitation change from 2000 to 2021 (C, D). Regional greening occurred in areas with an FVC increase, while browning appeared in areas with an FVC decrease (A). Over the past two decades, the world has been warming and greening. In particular, compared with the warming since the industrial revolution, the recent two decades of warming were unprecedented (B).

challenging the quantification of climatic factors' contribution to global vegetation change. Hence, separating the impact of precipitation and temperature will help develop an integrated adaptation approach to mitigate climate change influences on vegetation and prevent or delay undesired vegetation shifts.[25]

On the other hand, the research on quantifying the impacts of temperature and precipitation on vegetation change has significant implications for vegetation-related disaster prevention.[26] The vegetation decrease caused by increasing temperature or decreasing precipitation corresponds to atmospheric aridity and soil drought,[27–29] respectively, whose tangible influence and management solutions consequently differ.[30,31] At the same time, regional hydrothermal conditions and vegetation coverage are critical for forming typical mountainous disasters.[32,33] Therefore, the research on climatic attribution of vegetation changes, especially abnormal changes, can contribute to disaster monitoring and risk prevention.[34,35]

More complex is not necessarily better in large-scale modeling of the relationship between vegetation change and climatic change. Thus, we propose an innovative index CRTP with explicit physical meaning to simplify the complex problem, aiming to provide a concise and standardized approach to judge which is the dominant growth-limiting factor among the water and thermal condition in the global vegetated regions, using meteorological reanalysis data and remote sensing vegetation data. Moreover, we adopt Random Forest (RF) classification algorithms to identify the main factors affecting CRTP and construct the correlation model between screened climatic factors and CRTP, by which the possible CRTP changes in multiple climate scenarios are projected. The innovative work will hopefully provide theoretical support for future ecosystem management and disaster prevention.

RESULTS

Global vegetation and climate change

The world has been greening and warming over the past two decades (Figure 1). Remote sensing data shows that the global FVC increases with an average rate of 0.1%/10a (Figure 1A). We found that 24.3% of the world was significantly greening, much larger than browning (3.8%), which was consistent with the previous research.[3] Particular attention should be paid to the apparent vegetation improvement in China and India, which accounted for most global greening. In addition, vegetation degradation occurred mainly in the Arabian Peninsula, Central Siberia, and the boundary between Europe and Asia.

The global temperature has increased remarkably since the industrial revolution (Figure 1B). Global warming was striking from 2000 to 2021 with an average rate of 0.32°C/10a, much higher than before the 2000s. The regions with the most significant warming (>0.6°C/10a) were primarily located in the high latitudes of the northern hemisphere, the sensitive areas to climate change (Figure 1C). In contrast, the temperature decreased slightly (>–0.2°C/10a) in some regions, such as the parts of West and South Asia.

By contrast, the regime of global annual precipitation change was more complex. The annual precipitation has increased insignificantly with a rate of 10 mm/10a over the past two decades (Figure 1D). On the one hand, the precipitation increased in 40.7% of the world, one-fifth of which was significant. The areas with the most significant increase in precipitation were mainly located in the Indian Peninsula, Southeast Asia, and the Eastern US. On the other hand, 58.1% of the world experienced a precipitation decline, with a fifth of significant changes. The most significant decrease in precipitation appeared in Central Africa, the Northern Territory in Australia, and most parts of South America.

Global CRTP distribution over the past two decades

Horizontal distribution

The CRTP distribution was illustrated in regions where climatic factors dominated the vegetation change from 2000 to 2021 to quantitatively evaluate how precipitation and temperature have influenced global vegetation change (Figure 2). Precipitation dominated vegetation change in more than 70% of the area with significant CRTP, half of which was simultaneously influenced by temperature. The other half was

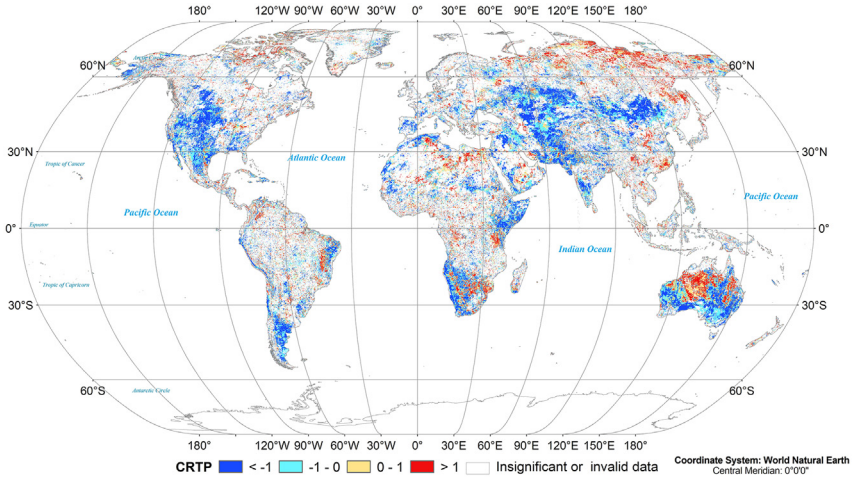

Figure 2. Global CRTP distribution from 2000 to 2021

The CRTP is an index comparing the relative contribution of temperature and precipitation to vegetation change within a certain period. The vegetation change in the color-covered areas in this figure is dominated by climatic factors (including temperature, precipitation, wind speed, air pressure, evaporation, and potential evaporation). The blank area indicates that CRTP is not statistically significant or data is missing in this region.

entirely controlled by precipitation. By contrast, the temperature was the dominant climatic factor affecting less than 30% of the vegetation change, with nearly 95% concurrently affected by precipitation.

In the meantime, the same type of CRTP tended to spatial aggregation. Regions with vegetation change dominated by temperature were distributed mainly in the high northern latitudes (north of 60 °N) and the Northern Territory in Australia. Although precipitation-dominated vegetation primarily appeared in the low and middle latitudes (between 60 °S and 60 °N), especially in southwestern North America, Central Asia, the Mongolian Plateau, and the southern regions of South America, Africa, and Australia.

Three-dimensional distribution

Although the global CRTP distribution seemed chaotic from 2000 to 2021, the spatial differentiation of climate-driving forces follows a regular pattern to a certain degree. The CRTP distribution varied significantly with longitude, latitude, and altitude (Figure 3).

Firstly, the dominant CRTP types differed significantly with longitudes or distances from the sea (Figure 3A). In particular, the proportion of negative CRTP increased first and then decreased eastward and westward from 30 °W, the rough boundary between the African-Eurasian and American continents, indicating the apparent decrease of the precipitation's influence on FVC change from the coast to inland areas. Besides, CRTP varied significantly with latitude because of the differentiation in heat conditions and radiation. Vegetation coverage in cold regions was more sensitive to the warming climate, like high latitudes and altitudes. Take the FVC change in the northern hemisphere as an example (Figure 3B). The influence of temperature on vegetation change overwhelmed precipitation in high latitudes (north of 60 °N), the relatively cold regions. By contrast, precipitation dominated the vegetation change in the middle and low latitudes, the relatively warm areas.

However, there was no significant proportions pattern of the four types of CRTP at different altitudes on the global scale (Figure 3C), indicating the complex impacts of elevation on climate factors.

CRTP classification model and projected global CRTP distribution

CRTP classification model

The CRTP distribution showed remarkable spatial regularity. So, it is feasible to explore its influencing factors and build related models. Based on the RF method, we here constructed the CRTP classification model according to climatic, geographic, and environmental factors and displayed the accuracy of classification models with different sets of input variables (Table 1). Among the thirteen models, Model 1, based on only temperature and precipitation, can achieve 59.89% accuracy. Then, we gradually added new variables with these two climatic

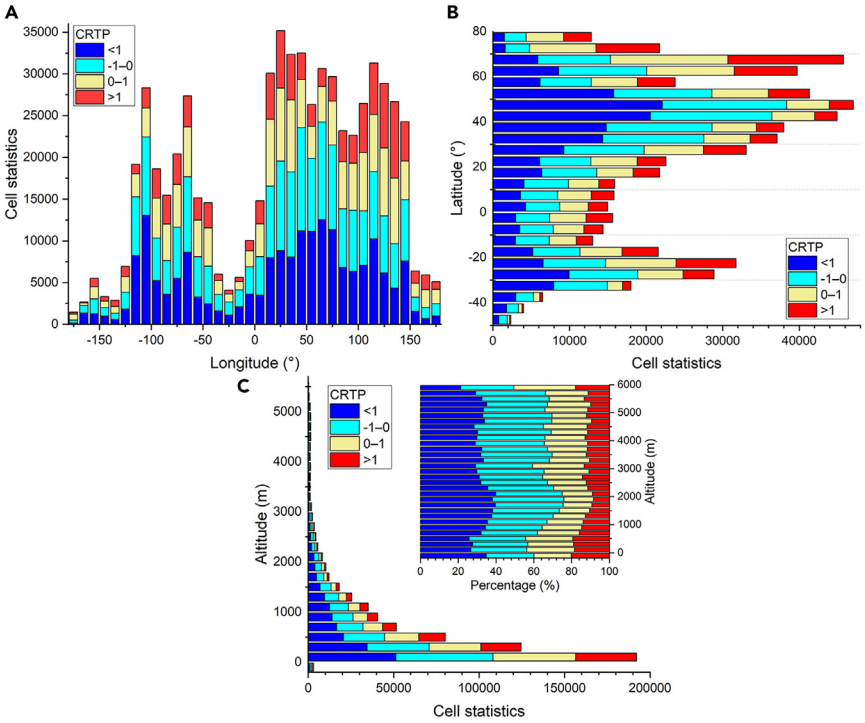

Figure 3. Three-dimensional distribution of CRTP

Variation of CRTP with longitude (A), latitude (B), and altitude (C). Here the cell statistics indicate the grid numbers corresponding to different CRTP types. Figure 3C displays the change in the proportion of different CRTP types with altitude. Longitudes, latitudes, and altitudes affect the CRTP via water vapor, heat, and hydrothermal conditions, respectively.

factors to form new models (Models 2 to 13). Finally, the optimal model with only climatic variables (i.e., temperature, precipitation, wind speed, air pressure, and evaporation) was Model 4 (accuracy: 65.22%).

In addition, we found that the model could be optimized significantly with more geographic and environmental information variables introduced (Table 1). As a result, the model accuracy improved remarkably, ranging from 65.98% (Model 7) to 66.61% (Model 9) with geographic variables (i.e., longitude, latitude, altitude, and distance from the sea) continually input (Models 7 to 10). This phenomenon further confirms our conclusions about the impacts of longitude, latitude, and altitude on CRTP distribution (Figure 3). Furthermore, the introduction of environmental variables (i.e., FVC and LUCC) also improved the model accuracy (Models 11 to 13), with the FVC alone behaving best (Model 11).

To summarize, the optimal classification model was Model 11, with an accuracy of 67.07% and a kappa coefficient of 0.54. According to the error matrix of Model 11 (Table 2), the classification accuracy of Type 4 was the highest (75.0%), with Type 2 the lowest (58.5%). Besides, the dominant climatic factor affecting FVC was precipitation in Type 1 and Type 2, whereas in Type 3 and Type 4 was temperature. Notably, this RF Model had high accuracy (88.7%) in distinguishing the dominant climatic factors to vegetation change.

However, we gave up the optimal classification Model 11 in the CRTP prediction because the future FVC and the land cover type are hard to predict. Instead, we screened Model 9, the optimal climate-geography model, for prediction, comprehensively considering the input variable's availability and reliability and the RF classifier's accuracy.

Projected global CRTP distribution

Based on the CRTP classification model, we can predict the CRTP distribution using future projections of multiple input variables. Here, we input CMIP6 climate projection with a resolution of 100 km into the

Table 1. Thirteen representative RF models with different input variables and their corresponding accuracy and kappa coefficient

Input variables		RF Model												
Category	Variable[a]	1	2	3	4	5	6	7	8	9	10	11	12	13
Climate[a]	Temperature	×	×	×	×	×	×	×	×	×	×	×	×	×
	Precipitation	×	×	×	×	×	×	×	×	×	×	×	×	×
	Wind speed		×	×	×	×	×	×	×	×	×	×	×	×
	Air pressure			×	×	×	×	×	×	×	×	×	×	×
	Evaporation				×		×	×	×	×	×	×	×	×
	Potential evaporation					×	×							
Geography	Longitude							×	×	×	×	×	×	×
	Latitude							×	×	×	×	×	×	×
	Altitude								×		×			
	Distance from sea									×	×	×	×	×
Environment	FVC[b]											×		×
	LUCC												×	×
	Accuracy (%)	59.89	64.15	64.62	65.22	65.13	65.06	65.98	66.18	66.61	66.45	67.07	66.49	66.7
	Kappa coefficient	0.44	0.50	0.50	0.51	0.51	0.51	0.52	0.53	0.53	0.53	0.54	0.53	0.53

[a]Each set of climatic variables (temperature, precipitation, wind speed, air pressure, evaporation, and potential evaporation) consists of climatic factors' average value and change rate. Environmental variables (FVC and LUCC) represent multi-year averages. The symbol × identifies the variables selected in each model.
[b]FVC here represents the average FVC from 2000 to 2021 in each sample.

CRTP classification model to predict the global CRTP distribution. We predicted the CRTP distribution under four SSP scenarios (i.e., SSP 1–2.6, SSP 2–4.5, SSP 3–7.0, and SSP 5–8.5) from 2021 to 2080 (Figures 4A–4F). Limited by the length of the sample sequence selected for model construction (22 years), we divided the future sixty years into three 20-year periods (2021–2040; 2041–2060; 2061–2080) (Figure 4H) and discussed the impact of temperature and precipitation on vegetation within different periods.

We could find one roughly zonal dividing line between the negative and positive values of projected global CRTP distribution. Consistent with the past two decades, precipitation will remain the predominant climatic factor influencing vegetation change in most of the world in the coming six decades (Figures 4A–4F). The precipitation will predominate vegetation changes in middle and low latitudes, whereas the temperature will dominate in high latitudes.

Moreover, the proportion of negative CRTP will decrease with higher radiative forcings. For example, precipitation will dominate the vegetation change in about 82% of the world from 2041 to 2060 in SSP 1–2.6, the scenario representing sustainable development in the future (Figure 4E). However, the corresponding proportion will reduce sharply to 66% in SSP 5–8.5, assuming an energy-intensive, fossil-based economy (Figure 4F). Simultaneously, vegetation change dominated by precipitation in SSP 1–2.6 will be replaced by temperature in SSP 5–8.5 in many regions, such as Southeast Asia, West and Central Africa, and north-central Australia. Consequently, the dividing line between the negative and positive CRTP values from 2041 to 2060 in SSP 5–8.5 will move southward significantly compared to SSP 1–2.6 (Figures 4E and 4F).

Equally significantly, the global distribution of CRTP will vary greatly in different periods (Figures 4A–4F, 4H). For instance, the proportion of temperature-dominated vegetation change will decrease over time in SSP 2–4.5 and SSP 3–7.0, contrasting with the increase in SSP 5–8.5 (Figure 4H). Besides, the disparities between the CRTP proportion in SSP 1–2.6 and SSP 5–8.5 will be the least significant within 2021–2040 because of the insignificant temperature variation between these scenarios (Figure 4G). Nevertheless, the discrepancies in CRTP proportion will gradually amplify over time (Figure 4H) as the global temperature difference between the four climate scenarios increases (Figure 4G). Therefore, the difference in CRTP proportion between the low and high radiative forcing scenarios will reach its maximum from 2061 to 2080 (Figure 4H).

Table 2. CRTP classification error matrix of Model 11, the optimal RF model

	Reference						
Prediction	Type 1	Type 2	Type 3	Type 4	Accuracy	Dominant factor	Accuracy[a]
Type 1	3096	1222	217	72	67.2%	Temperature dominated	88.7%
Type 2	1561	4547	1397	264	58.5%		
Type 3	363	1850	8621	2747	63.5%	Precipitation dominated	
Type 4	81	331	3174	10778	75.0%		

[a]Accuracy here distinguishes the dominant climatic factors (temperature or precipitation) to vegetation change.

DISCUSSION

What modulates the CRTP distribution

The construction and rationality of CRTP

Temperature and precipitation dominate the vegetation change in many parts of the world to some degree.[12,13] Furthermore, many studies have pointed out that the impact of these two factors on vegetation varies significantly in different regions.[12,17,18,20] However, a reliable strategy to quantitatively distinguish whether temperature or precipitation dominates vegetation change in a specific region is still lacking. One of the first difficulties in giving this strategy is that the relationship between temperature, precipitation, and vegetation is quite complex.[24] Hence, an index is urgently needed to simplify this complex relationship and quantitatively compare the contribution of temperature and precipitation to vegetation change. The relative contribution is one of the most widely used indexes to separate the impact of different factors on vegetation change.[36–38] Hence, we constructed the innovative index by comparing the relative contribution of temperature and precipitation to FVC change. Moreover, we considered other important climatic factors (e.g., wind speed, air pressure, evaporation, and potential evaporation) when calculating the relative contribution using ANOVA to extract a more realistic individual impact of temperature or precipitation. With the index CRTP, we could initially display the intuitive global distribution of the dominance between temperature and precipitation influencing vegetation change.

Notably, the distribution of the dominance between temperature and precipitation from 2000 to 2021 described by CRTP was highly consistent with existing research conclusions, largely verifying the rationality of this index. Firstly, temperature dominated the FVC change in the northern hemisphere's high latitudes, compared with the dominance of precipitation in the relatively low latitudes (Figure 2), corresponding with the previous research.[12] Although on a smaller scale, precipitation dominated the vegetation change in most Mongolian Plateau, corresponding to the regional greening caused by increasing rainfall.[39] Besides, precipitation and drought are projected to be the most critical factors in most temperate deserts of Central Asia in the 21st century,[40] which is also clearly displayed by CRTP. Furthermore, unlike existing research, CRTP provides a normative and quantitative scheme to distinguish the dominant factor affecting FVC between temperature and precipitation at different scales. Equally importantly, referring to the construction roadmap of CRTP, we can develop similar parameters related to other environmental indicators, such as phenology, biomass, or biodiversity, which will provide new strategies and methods for research in these fields, hopefully providing more comprehensive theoretical support for ecosystem management. Finally, given the innovative index's concise physical meaning, practical application, and low barrier to utilization, we hope that CRTP and other relevant indexes initiated soon are worth popularization and could be developed into a widely used tool for studies related to climate and its ecological impacts.

Factors affecting CRTP distribution

We preliminarily filtered the factors that affect CRTP and screen the optimal RF classification Model 11 (Table 1). Then, taking Model 11 as an example, we could discuss the relative contribution of input variables to CRTP classification based on the ranking of normalized variable importance (Figure 5).

There were six factors with normalized variable importance larger than one, including three climatic and three geographic variables. Among these, annual average temperature ranked first. The three most critical climatic variables contributing to CRTP classification were annual average temperature, temperature change, and annual precipitation, which could roughly describe regional hydrothermal conditions.

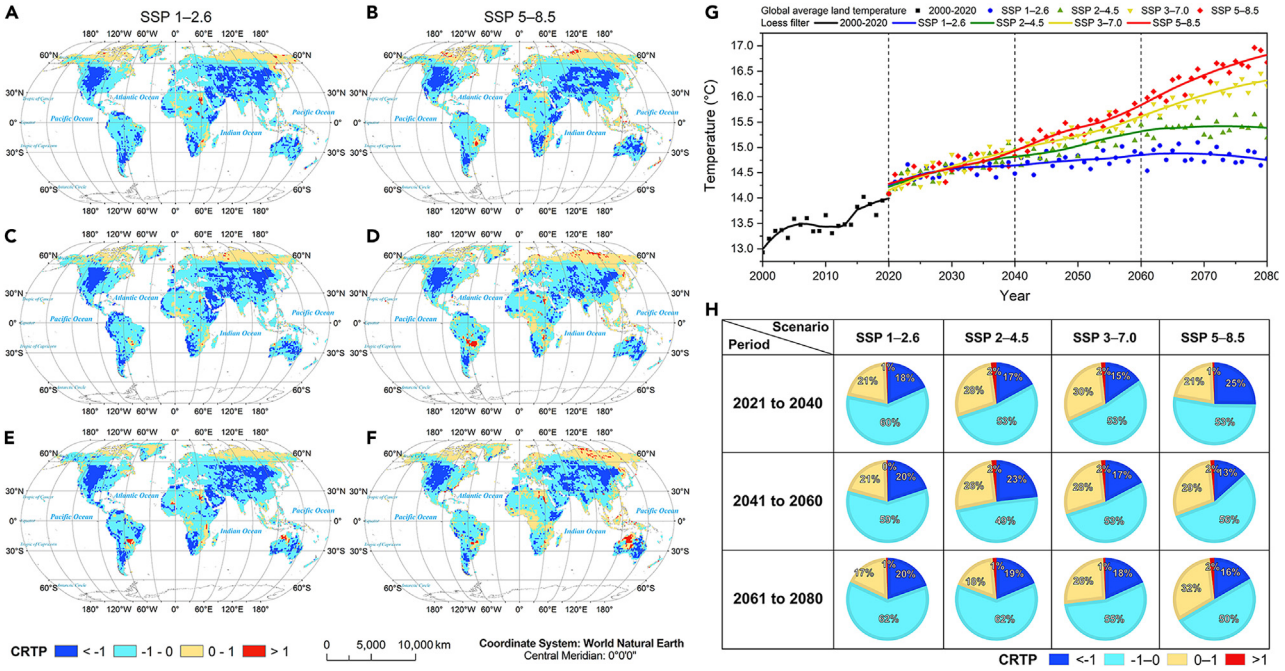

Figure 4. CRTP projection over the next 60 years

(A–F) Projected future CRTP distribution in SSP 1–2.6 and SSP 5–8.5 from (A, B) 2021 to 2040, (C, D) 2041 to 2060, and (E, F) 2061 to 2080.

(G) Temperature projection in different scenarios in CMIP 6 models. The black square dots and curves in Figure 4G represent the actual global temperature change from 2000 to 2020 based on ERA5 data. The blue, green, yellow, and red dots and curves show the temperature projection in the future 60 years in different scenarios.

(H) The proportion of different types of CRTP in different scenarios and periods. Precipitation will remain the dominant climatic factor affecting vegetation change in most of the world. The contributions of temperature to vegetation change will increase with radiative forcing over time.

Besides, the importance of all the geographic variables input to the model was considerable, with latitude and longitude ranking second and third, respectively.

This result corresponded well with the previous research conclusions. On the one hand, the relationship between vegetation and temperature/precipitation varied regularly with latitude and longitude.[12,41] On the other hand, the spatial differences of the dominant climatic factors affecting vegetation depended on the heterogeneity of hydrothermal conditions and the magnitudes of climate change.[24,42] Comprehensively considering the six critical factors affecting CRTP, we can conclude that CRTP distribution will change locally with climate and environment under a relatively fixed distribution pattern determined by longitude and latitude.

Notably, three variables (i.e., potential evaporation, altitude, and LUCC) were involved in the model simulation but not adopted in the optimal Model 11 (Table 1). Firstly, we found that the evaporation and potential evaporation had similar effects on improving the model accuracy (Models 4 and 5) while simultaneously inputting these two factors would reduce the model accuracy (Model 6) (Table 1). However, potential evaporation in the ERA5-land dataset is computed as open-water evaporation, differing from the potential evapotranspiration predicted in the CMIP 6 data. Therefore, we selected total evaporation (including sublimation and transpiration) as the last input climatic variable.

Secondly, altitude contributed less to CRTP distribution than latitude and longitude, well corresponding to the three-dimensional differentiation of CRTP (Figure 3). We proposed that altitude indirectly affected the CRTP distribution through other factors, such as temperature, precipitation, and terrain. In addition, the influence tends to be scale-dependent.[17,43] So, the effects of altitude on CRTP seem challenging to describe quantitatively (Figure 3).

Finally, land use cover/change also significantly impacted regional CRTP type. Nevertheless, LUCC seemed to become a secondary substitute in the simulation. We have excluded the regions related to

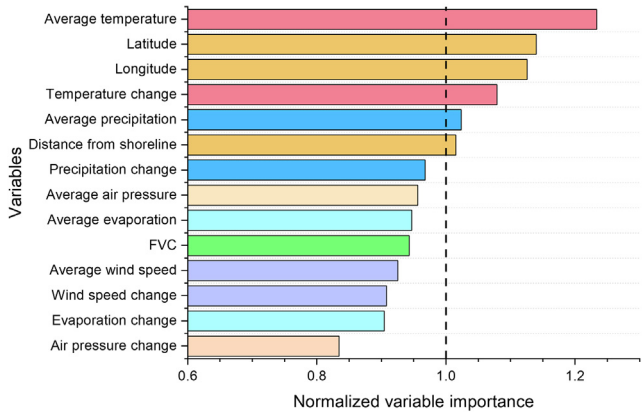

Figure 5. Normalized variable importance of all input variables in Model 11

The variables with the same color represent the same type of climatic, geographic, or environmental factors. There are six factors with normalized variable importance larger than one, including three climatic and three geographic variables.

human activities from samplings in the model simulation. At the same time, the remaining LUCC information of natural land can be extracted from remote sensing images and almost covered in FVC.[44,45]

CRTP's application in vegetation degradation monitoring

Although global vegetation was generally improving because of the warming and CO_2 fertilization,[46] regional vegetation degradation may reduce ecosystem services and health, especially in dryland. Therefore, we used the index CRTP to discuss the impacts of hydrothermal condition change on global vegetation degradation. Here, we identified the areas with the most significant vegetation degradation in different continents based on FVC change (Figure 6).

Climate change, particularly precipitation (CRTP<0), led to regional vegetation degradation in North America, especially in southeast Canada (Figure 6A). During the past few decades, the increasing impact of warm droughts reduced plant productivity and carbon sequestration in North America.[47,48] Furthermore, rapid climate change promoted vegetation conversion, including trees to savannas and grasslands, accounting for decreased vegetation coverage.[49]

Although in Europe and Asia, vegetation changes in dryland were mixed with regions experiencing vegetation improvement and degradation.[50,51] The vegetation degradation around the boundary between Europe and Asia was primarily distributed in Russia and the Volga Federal District regions in eastern Kazakhstan with negative CRTP, meaning the declined precipitation was responsible for this phenomenon (Figure 6B). We also found the vegetation browning in higher latitudes in Central Siberia Highlands with a mainly positive CRTP (Figure 6C). This phenomenon well corresponded to the degradation of grasslands[52] and boreal forests[53] in many regions of Asia during recent decades caused by drought and overgrazing.[53,54]

Besides, vegetation coverage decreased remarkably in some desert regions in low latitudes with positive CRTP as a result of increasing evaporation with warming temperatures, especially in northern Africa and the Arabian Peninsula in Asia (Figure 6D). Moreover, it is worth noting that decreasing precipitation led to vegetation loss on the west coast in the middle and low latitudes (CRTP<0) (15°S to 45°S) of Africa and South America (Figures 6E and 6F). Research suggested that these regions' precipitation reduction might be related to the variation of radiative forcing[55] and ENSO.[56]

In addition, although widespread greening was found over much of Australia because of wetter conditions,[57] there were still large areas with decreasing vegetation affected by droughts.[58] Current research emphasizes precipitation's dominant role in the dryland's dramatic vegetation change.[59] The CRTP distribution verified that regional drying resulted in vegetation degradation in Western Australia in the past two decades (Figure 6G). At the same time, vegetation coverage decreased in north-central Australia

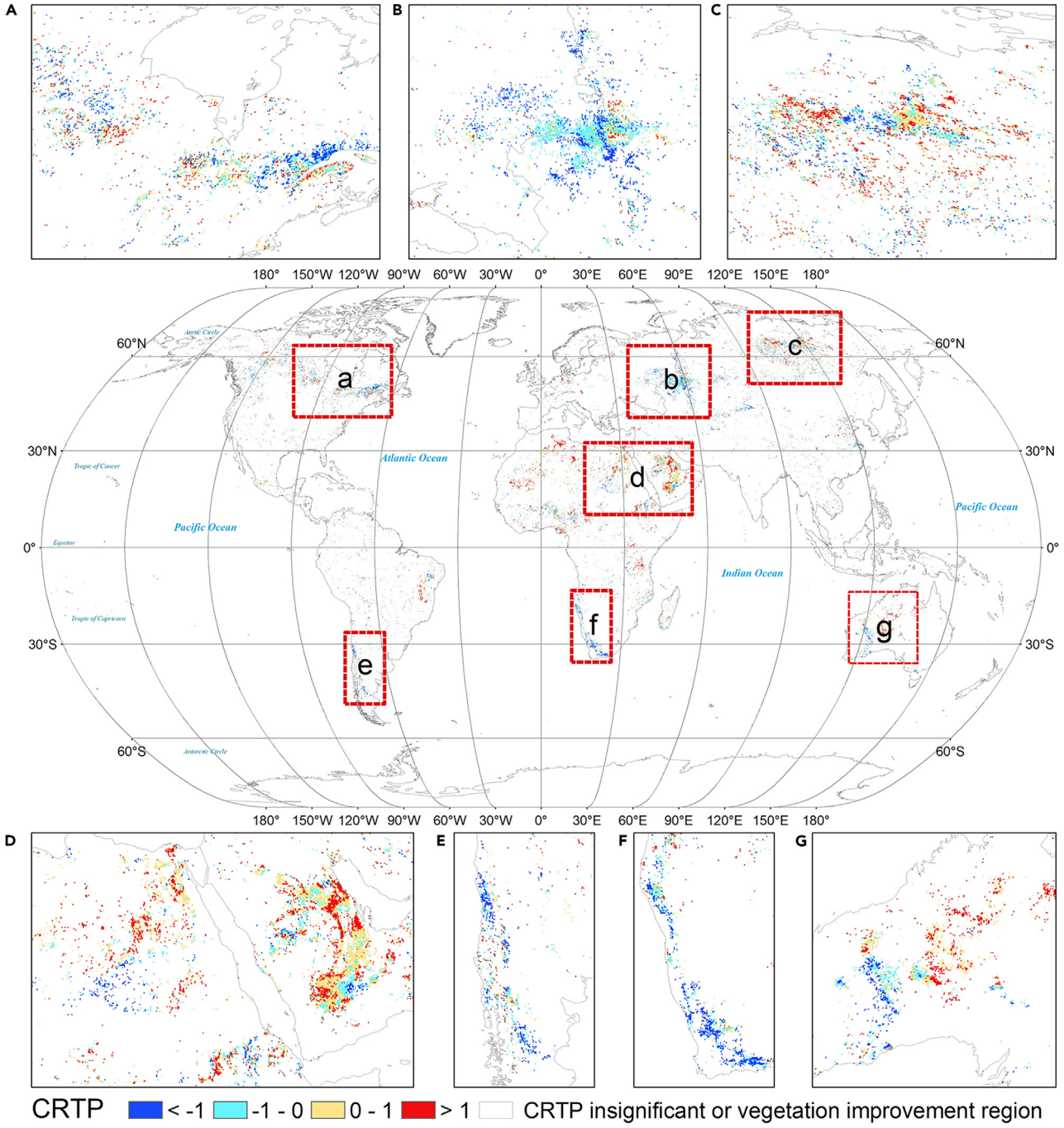

Figure 6. CRTP distribution in areas with significant vegetation degradation from 2000 to 2021

(A–G) In this figure, the vegetation degradation responds to the FVC decrease in Figure 1; red dotted frames indicate seven regions with the most significant vegetation degradation in each continent; Figures 6A–6G zoom in on the areas in the red dotted frames and demonstrate the spatial distribution of degradation in detail. Over the past two decades, precipitation decline accounts for the vegetation degradation in North America, the boundary between Europe and Asia, and the west coast of the southern hemisphere. Meanwhile, warming temperature or anthropogenic perturbance contributes to the vegetation decrease in Arabian Peninsula, northern Africa, central Siberia Highlands, and north-central Australia.

because of dramatic warming. Under similar climatic warming and drying conditions, the magnitude of temperature and precipitation change will jointly determine the vegetation growth-limiting factor in Australia.

In short, the index CRTP can help make quick climatic attribution when discussing regional desertification or vegetation degradation. However, if the vegetation change mechanism explained by CRTP could not match the actual climate change, a disturbance of non-climatic factors, such as anthropogenic activities and natural hazards, should be taken into consideration.

CRTP's application in disaster prevention and ecosystem management

In the context of continued warming, losses from natural disasters, including extreme weather events and mountain hazards, have increased intensely over the last decades.[60] More and more adaptation evidence has disclosed that both seasonal and dynamic forecast and ecosystem-based and climate-adaptive management are feasible and effective.[61–63] CRTP projections are expected to make contributions to ecosystem management and disaster prevention. Here, we took drought prevention and forest management as examples for further discussion.

Utilization in drought prevention

Soil drought and atmospheric aridity are considered the leading cause of desertification aggravation in many regions worldwide, whereas different types of drought correspond to diversified consequences and climatic conditions.[28,64] The soil drought emphasizes the low soil moisture content, mainly in areas with a prolonged lack of precipitation.[27,29] Although the high atmospheric vapor pressure deficit, an essential indicator of atmospheric aridity, often is accompanied by high temperatures and low relative humidity.[65] Different types of drought restrictions on vegetation productivity vary significantly.[66] Moreover, scholars have assessed the relative contribution of water availability and temperature to the ecosystem based on the limitation analysis of different drought types on carbon flux.[67]

Here, we can use reverse thinking first to judge the dominant climatic factors leading to vegetation change in arid areas and then infer the regional drought type to a certain extent. This method should be effective in the prediction of drought-type conversion. For example, regions with positive CRTP will expand over time under SSP 5–8.5 in some arid areas, such as southern Africa and south-central Australia, implying the regional drought type will change from soil drought to atmospheric aridity. The corresponding prevention and management will differ with drought types.[30] Hence, our research will provide theoretical support for regional drought prevention in the future.

Utilization in forest management

Research on the dominant climatic factor affecting vegetation change has significant implications for ecosystem management.[21,22] Hence, separating the impact of precipitation and temperature will help develop an integrated adaptation approach to mitigate climate change influences on vegetation and prevent or delay undesired vegetation shifts.[25]

Projected temperature and precipitation change will have potentially negative consequences for the forest ecosystem, such as increasing wildfire,[23,68] decreasing biodiversity,[6] and insect and pathogen outbreaks.[69] Furthermore, the vulnerability of forest ecosystems to climate change is shifting rapidly against the backdrop of global warming.[70,71] However, appropriate ecosystem management can help mitigate climate change impacts on vegetation[25] and restrain the occurrence of disasters.[72]

Reasonable forest management alternatives based on future climate projections are of great significance in conserving biodiversity,[73] mitigating biospheric greenhouse gas emissions,[22] and reducing the wildfire risk,[74] which highly depends on the climate and vegetation change pattern.[22,75] According to CRTP projection, we could monitor the global vegetation change and analyze its climatological attribution. Therefore, regional vegetation fluctuation's ecological instability or disaster risk could be monitored, predicted, and controlled. Risky vegetation change, such as an abnormal increase in vegetation coverage with positive CRTP in regions at high risk of wildfire, should be real-time monitored and warned early.

Limitations of the study

The study limitations in the optimal model and CRTP prediction are summarized below.

First, the response of vegetation to temperature and precipitation was complex.[24] Except for existing factors adopted in our model, many other factors such as CO_2,[46,76] vegetation species,[6] and tree age[77] also

influenced the vegetation response to climate change. Although it is unrealistic to consider all possible driving forces in one model, the model accuracy may be further improved with all these factors covered.

Second, we screened the samples and artificially filtered out the impact of human activities in the simulation and prediction. However, human activities like logging, farming, ecological management, and afforestation had multiple (positive or negative) effects on regional vegetation.[3,78,79] Therefore, if we can solve the bottleneck problem that human activities are challenging to quantify and predict, we will establish a better prediction model that comprehensively considers natural and human factors.

Besides, there were certain limitations and deficiencies in describing the global CRTP distribution using a single model. Hence, it might be an excellent method to improve the simulation's accuracy to classify the global samples according to specific indicators, such as vegetation types, and then construct models independently under different classifications.

Finally, the low spatial resolution of CMIP6 data accounted for the uncertainty of CRTP prediction, especially for the absolute value of CRTP larger than one. These two kinds of CRTP usually correspond to a relatively extreme temperature or precipitation. However, prediction data with a low resolution could not provide local information about extremely low or high climates. Hence, high-resolution climate prediction is necessary to improve prediction accuracy.

STAR★METHODS

Detailed methods are provided in the online version of this paper and include the following:

- KEY RESOURCES TABLE
- RESOURCE AVAILABILITY
  - Lead contact
  - Materials availability
  - Data and code availability
- METHOD DETAILS
  - Climatic and environmental data
  - CMIP6 simulations
  - FVC calculation
  - Trend of vegetation and climate change
  - CRTP calculation and classification
  - Random forest optimal model for CRTP classification and prediction

ACKNOWLEDGMENTS

This work was supported by the Strategic Priority Research Program of the Chinese Academy of Sciences (XDA23090302), the Second Tibetan Plateau Scientific Expedition and Research Program (STEP) (2019QZ KK0903), and the Strategic Priority Research Program of the Chinese Academy of Sciences (XDA20030203).

AUTHOR CONTRIBUTIONS

X.Z. and X.L. conceived the research and designed this index. X.L. conducted the data processing, model operation, and statistical analysis. X.Z. and X.L. drew the graphs, wrote the manuscript, and revised the manuscript.

DECLARATION OF INTERESTS

The authors declare that they have no known conflict of interest.

INCLUSION AND DIVERSITY

We support inclusive, diverse, and equitable conduct of research.

Received: November 28, 2022
Revised: March 12, 2023
Accepted: May 23, 2023
Published: May 26, 2023

REFERENCES

1. Cao, M., and Woodward, F.I. (1998). Dynamic responses of terrestrial ecosystem carbon cycling to global climate change. Nature *393*, 249–252. https://doi.org/10.1038/30460.

2. Vygodskaya, N.N., Groisman, P.Y., Tchebakova, N.M., Kurbatova, J.A., Panfyorov, O., Parfenova, E.I., and Sogachev, A.F. (2007). Ecosystems and climate interactions in the boreal zone of northern Eurasia. Environ. Res. Lett. *2*, 045033–045037. https://doi.org/10.1088/1748-9326/2/4/045033.

3. Chen, C., Park, T., Wang, X., Piao, S., Xu, B., Chaturvedi, R.K., Fuchs, R., Brovkin, V., Ciais, P., Fensholt, R., et al. (2019). China and India lead in greening of the world through land-use management. Nat. Sustain. *2*, 122–129. https://doi.org/10.1038/s41893-019-0220-7.

4. Lin, D., Xia, J., and Wan, S. (2010). Climate warming and biomass accumulation of terrestrial plants: a meta-analysis. New Phytol. *188*, 187–198. https://doi.org/10.1111/j.1469-8137.2010.03347.x.

5. Peñuelas, J., Rutishauser, T., and Filella, I. (2009). Phenology feedbacks on climate change. Science *324*, 887–888. https://doi.org/10.1126/science.1173004.

6. Antão, L.H., Bates, A.E., Blowes, S.A., Waldock, C., Supp, S.R., Magurran, A.E., Dornelas, M., and Schipper, A.M. (2020). Temperature-related biodiversity change across temperate marine and terrestrial systems. Nat. Ecol. Evol. *4*, 927–933. https://doi.org/10.1038/s41559-020-1185-7.

7. Peñuelas, J., and Filella, I. (2001). Responses to a warming world. Science *294*, 793–795. https://doi.org/10.1126/science.1066860.

8. Westerling, A.L., Gershunov, A., Brown, T.J., Cayan, D.R., and Dettinger, M.D. (2003). Climate and wildfire in the western United States. Bull. Am. Meteorol. Soc. *84*, 595–604. https://doi.org/10.1175/BAMS-84-5-595.

9. Zhang, Y., and Steiner, A.L. (2022). Projected climate-driven changes in pollen emission season length and magnitude over the continental United States. Nat. Commun. *13*, 1234. https://doi.org/10.1038/s41467-022-28764-0.

10. Malhi, Y., Aragão, L., Galbraith, D., Huntingford, C., Fisher, R., Zelazowski, P., Sitch, S., Mcsweeney, C., and Meir, P. (2009). Exploring the likelihood and mechanism of a climate-change-induced dieback of the Amazon rainforest. Proc. Natl. Acad. Sci. USA *106*, 20610–20615. https://doi.org/10.1073/pnas.0804619106.

11. Crick, H.Q.P., Dudley, C., Glue, D.E., and Thomson, D.L. (1997). UK birds are laying eggs earlier. Nature *388*, 526. https://doi.org/10.1038/41453.

12. Ichii, K., Kawabata, A., and Yamaguchi, Y. (2002). Global correlation analysis for NDVI and climatic variables and NDVI trends: 1982-1990. Int. J. Rem. Sens. *23*, 3873–3878. https://doi.org/10.1080/01431160110119416.

13. Overpeck, J.T., Rind, D., and Goldberg, R. (1990). Climate-induced changes in forest disturbance and vegetation. Nature *343*, 51–53. https://doi.org/10.1038/343051a0.

14. Piao, S., Fang, J., Ji, W., Guo, Q., Ke, J., and Tao, S. (2004). Variation in a satellite-based vegetation index in relation to climate in China. J. Veg. Sci. *15*, 219–226. https://doi.org/10.1658/1100-9233(2004)015[0219:VIASVI]2.0.CO;2.

15. Wang, J., Price, K.P., and Rich, P.M. (2001). Spatial patterns of NDVI in response to precipitation and temperature in the central Great Plains. Int. J. Rem. Sens. *22*, 3827–3844. https://doi.org/10.1080/01431160010007033.

16. Peng, J., Dong, W., Yuan, W., and Zhang, Y. (2012). Responses of grassland and forest to temperature and precipitation changes in Northeast China. Adv. Atmos. Sci. *29*, 1063–1077. https://doi.org/10.1007/s00376-012-1172-2.

17. Tao, J., Xu, T., Dong, J., Yu, X., Jiang, Y., Zhang, Y., Huang, K., Zhu, J., Dong, J., Xu, Y., and Wang, S. (2018). Elevation-dependent effects of climate change on vegetation greenness in the high mountains of southwest China during 1982-2013: elevation-dependent effects of climate change on vegetation greenness. Int. J. Climatol. *38*, 2029–2038. https://doi.org/10.1002/joc.5314.

18. Fabricante, I., Oesterheld, M., and Paruelo, J.M. (2009). Annual and seasonal variation of NDVI explained by current and previous precipitation across Northern Patagonia. J. Arid Environ. *73*, 745–753. https://doi.org/10.1016/j.jaridenv.2009.02.006.

19. Zhang, G., Xu, X., Zhou, C., Zhang, H., and Ouyang, H. (2011). Responses of vegetation changes to climatic variations in hulun buir grassland in past 30 years. Acta Geograph. Sin. *66*, 47–58. https://doi.org/10.3724/SP.J.1011.2011.00415.

20. Sun, J., Qin, X., and Yang, J. (2016). The response of vegetation dynamics of the different alpine grassland types to temperature and precipitation on the Tibetan Plateau. Environ. Monit. Assess. *188*, 20. https://doi.org/10.1007/s10661-015-5014-4.

21. Bright, R.M., Antón-Fernández, C., Astrup, R., Cherubini, F., Kvalevåg, M., and Strømman, A.H. (2013). Climate change implications of shifting forest management strategy in a boreal forest ecosystem of Norway. Global Change Biol. *20*, 607–621. https://doi.org/10.1111/gcb.12451.

22. Obersteiner, M., Böttcher, H., and Yamagata, Y. (2010). Terrestrial ecosystem management for climate change mitigation. Curr. Opin. Environ. Sustain. *2*, 271–276. https://doi.org/10.1016/j.cosust.2010.05.006.

23. Williams, A.P., Allen, C.D., Millar, C.I., Swetnam, T.W., Michaelsen, J., Still, C.J., and Leavitt, S.W. (2010). Forest responses to increasing aridity and warmth in the southwestern United States. Proc. Natl. Acad. Sci. USA *107*, 21289–21294. https://doi.org/10.1073/pnas.0914211107.

24. Seddon, A.W.R., Macias-Fauria, M., Long, P.R., Benz, D., and Willis, K.J. (2016). Sensitivity of global terrestrial ecosystems to climate variability. Nature *531*, 229–232. https://doi.org/10.1038/nature16986.

25. Scheiter, S., and Savadogo, P. (2016). Ecosystem management can mitigate vegetation shifts induced by climate change in West Africa. Ecol. Model. *332*, 19–27. https://doi.org/10.1016/j.ecolmodel.2016.03.022.

26. Rocca, M.E., Brown, P.M., Macdonald, L.H., and Carrico, C.M. (2014). Climate change impacts on fire regimes and key ecosystem services in Rocky Mountain forests. For. Ecol. Manage. *327*, 290–305. https://doi.org/10.1016/j.foreco.2014.04.005.

27. Hohenegger, C., Brockhaus, P., Bretherton, C.S., and Schär, C. (2009). The soil moisture–precipitation feedback in simulations with explicit and parameterized convection. J. Clim. *22*, 5003–5020. https://doi.org/10.1175/2009JCLI2604.1.

28. Qing, Y., Wang, S., Ancell, B.C., and Yang, Z.-L. (2022). Accelerating flash droughts induced by the joint influence of soil moisture depletion and atmospheric aridity. Nat. Commun. *13*, 1139. https://doi.org/10.1038/s41467-022-28752-4.

29. Sheffield, J. (2004). A simulated soil moisture based drought analysis for the United States. J. Geophys. Res. *109*, D24108. https://doi.org/10.1029/2004JD005182.

30. Farooq, M., Wahid, A., Kobayashi, N., Fujita, D., and Basra, S.M.A. (2009). Plant drought stress: effects, mechanisms and management. Agron. Sustain. Dev. *29*, 185–212. https://doi.org/10.1051/agro:2008021.

31. Wouters, H., Keune, J., Petrova, I.Y., van Heerwaarden, C.C., Teuling, A.J., Pal, J.S., Vilà-Guerau de Arellano, J., and Miralles, D.G. (2022). Soil drought can mitigate deadly heat stress thanks to a reduction of air humidity. Sci. Adv. *8*, eabe6653. https://doi.org/10.1126/sciadv.abe6653.

32. Rickli, C., and Graf, F. (2009). Effects of forests on shallow landslides - case studies in Switzerland. For. Snow Landsc. Res. *82*.

33. Zou, Q., Cui, P., Jiang, H., Wang, J., Li, C., and Zhou, B. (2020). Analysis of regional river blocking by debris flows in response to climate change. Sci. Total Environ. *741*, 140262. https://doi.org/10.1016/j.scitotenv.2020.140262.

34. Chen, X., Cui, P., and Wei, F. (2006). Study of control debris flow in high-covered vegetation region. J. Mt. Sci. *24*, 333–339. https://doi.org/10.1016/S1872-2040(06)60004-2.

35. Jacquemart, M., and Tiampo, K. (2020). Radar Coherence and NDVI Ratios as Landslide

Early Warning Indicators. https://doi.org/10.5194/nhess-2020-227.

36. Huang, S., Zheng, X., Ma, L., Wang, H., Huang, Q., Leng, G., Meng, E., and Guo, Y. (2020). Quantitative contribution of climate change and human activities to vegetation cover variations based on GA-SVM model. J. Hydrol X. *584*, 124687. https://doi.org/10.1016/j.jhydrol.2020.124687.

37. Liu, H., Li, X., Mao, F., Zhang, M., Zhu, D., He, S., Huang, Z., and Du, H. (2021). Spatiotemporal evolution of fractional vegetation cover and its response to climate change based on MODIS data in the subtropical region of China. Rem. Sens. *13*, 913. https://doi.org/10.3390/rs13050913.

38. Mukhortova, L., Schepaschenko, D., Moltchanova, E., Shvidenko, A., Khabarov, N., and See, L. (2021). Respiration of Russian soils: climatic drivers and response to climate change. Sci. Total Environ. *785*, 147314. https://doi.org/10.1016/j.scitotenv.2021.147314.

39. Li, X., Zhang, X., and Xu, X. (2022). Precipitation and anthropogenic activities jointly green the China–Mongolia–Russia economic corridor. Rem. Sens. *14*, 187. https://doi.org/10.3390/rs14010187.

40. Zhang, C., Lu, D., Chen, X., Zhang, Y., Maisupova, B., and Tao, Y. (2016). The spatiotemporal patterns of vegetation coverage and biomass of the temperate deserts in Central Asia and their relationships with climate controls. Remote Sens. Environ. *175*, 271–281. https://doi.org/10.1016/j.rse.2016.01.002.

41. Lloyd, A.H., Bunn, A.G., and Berner, L. (2011). A latitudinal gradient in tree growth response to climate warming in the Siberian taiga: tree response to climate in the siberian taiga. Global Change Biol. *17*, 1935–1945. https://doi.org/10.1111/j.1365-2486.2010.02360.x.

42. Euskirchen, E.S., McGuire, A.D., Chapin, F.S., Yi, S., and Thompson, C.C. (2009). Changes in vegetation in northern Alaska under scenarios of climate change, 2003–2100: implications for climate feedbacks. Ecol. Appl. *19*, 1022–1043. https://doi.org/10.1890/08-0806.1.

43. Diodato, N. (2005). The influence of topographic co-variables on the spatial variability of precipitation over small regions of complex terrain. Int. J. Climatol. *25*, 351–363. https://doi.org/10.1002/joc.1131.

44. Han, K., Champeaux, J., and Roujean, J. (2004). A land cover classification product over France at 1 km resolution using SPOT4/VEGETATION data. Remote Sens. Environ. *92*, 52–66. https://doi.org/10.1016/j.rse.2004.05.005.

45. Kressler, F.P., and Steinnocher, K.T. (1999). Detecting land cover changes from NOAA-AVHRR data by using spectral mixture analysis. Int. J. Appl. Earth Obs. Geoinf. *1*, 21–26. https://doi.org/10.1016/S0303-2434(99)85024-7.

46. Kolby Smith, W., Reed, S.C., Cleveland, C.C., Ballantyne, A.P., Anderegg, W.R.L., Wieder, W.R., Liu, Y.Y., and Running, S.W. (2016). Large divergence of satellite and Earth system model estimates of global terrestrial CO2 fertilization. Nat. Clim. Change *6*, 306–310. https://doi.org/10.1038/nclimate2879.

47. Gampe, D., Zscheischler, J., Reichstein, M., O'Sullivan, M., Smith, W.K., Sitch, S., and Buermann, W. (2021). Increasing impact of warm droughts on northern ecosystem productivity over recent decades. Nat. Clim. Change *11*, 772–779. https://doi.org/10.1038/s41558-021-01112-8.

48. Mekonnen, Z.A., Grant, R.F., and Schwalm, C. (2017). Carbon sources and sinks of North America as affected by major drought events during the past 30 years. Agric. For. Meteorol. *244–245*, 42–56. https://doi.org/10.1016/j.agrformet.2017.05.006.

49. Bendixsen, D.P., Hallgren, S.W., and Frazier, A.E. (2015). Stress factors associated with forest decline in xeric oak forests of south-central United States. For. Ecol. Manage. *347*, 40–48. https://doi.org/10.1016/j.foreco.2015.03.015.

50. Miao, L., Moore, J.C., Zeng, F., Lei, J., Ding, J., He, B., and Cui, X. (2015). Footprint of research in desertification management in China. Land Degrad. Dev. *26*, 450–457.

51. Prăvălie, R., Patriche, C., and Bandoc, G. (2017). Quantification of land degradation sensitivity areas in Southern and Central Southeastern Europe. New results based on improving DISMED methodology with new climate data. Catena *158*, 309–320. https://doi.org/10.1016/j.catena.2017.07.006.

52. Prishchepov, A.V., Myachina, K.V., Kamp, J., Smelansky, I., Dubrovskaya, S., Ryakhov, R., Grudinin, D., Yakovlev, I., and Urazaliyev, R. (2021). Multiple trajectories of grassland fragmentation, degradation, and recovery in Russia's steppes. Land Degrad. Dev. *32*, 3220–3235. https://doi.org/10.1002/ldr.3976.

53. Berner, L.T., Beck, P.S.A., Bunn, A.G., Lloyd, A.H., and Goetz, S.J. (2011). High-latitude tree growth and satellite vegetation indices: correlations and trends in Russia and Canada (1982–2008). J. Geophys. Res. *116*, G01015. https://doi.org/10.1029/2010JG001475.

54. Chadaeva, V., Gorobtsova, O., Pshegusov, R., Tsepkova, N., Tembotov, R., Khanov, Z., Gedgafova, F., Zhashuev, A., Uligova, T., Khakunova, E., and Stepanyan, E. (2021). Stages of grassland degradation in subalpine ecosystems of the Central Caucasus, Russia. Chil. J. Agric. Res. *81*, 630–642. https://doi.org/10.4067/S0718-58392021000400630.

55. Shindell, D.T., Voulgarakis, A., Faluvegi, G., and Milly, G. (2012). Precipitation response to regional radiative forcing. Atmos. Chem. Phys. *12*, 6969–6982. https://doi.org/10.5194/acp-12-6969-2012.

56. Richard, Y., Trzaska, S., Roucou, P., and Rouault, M. (2000). Modification of the southern African rainfall variability/ENSO relationship since the late 1960s. Clim. Dynam. *16*, 883–895. https://doi.org/10.1007/s003820000086.

57. Damberg, L., and AghaKouchak, A. (2014). Global trends and patterns of drought from space. Theor. Appl. Climatol. *117*, 441–448. https://doi.org/10.1007/s00704-013-1019-5.

58. Donohue, R.J., Mcvicar, T.R., and Roderick, M.L. (2009). Climate-related trends in Australian vegetation cover as inferred from satellite observations, 1981-2006. Global Change Biol. *15*, 1025–1039. https://doi.org/10.1111/j.1365-2486.2008.01746.x.

59. Burrell, A.L., Evans, J.P., and Liu, Y. (2017). Detecting dryland degradation using time series segmentation and residual trend analysis (TSS-RESTREND). Remote Sens. Environ. *197*, 43–57. https://doi.org/10.1016/j.rse.2017.05.018.

60. Mechler, R., and Bouwer, L.M. (2015). Understanding trends and projections of disaster losses and climate change: is vulnerability the missing link? Clim. Change *133*, 23–35. https://doi.org/10.1007/s10584-014-1141-0.

61. Maina, J., Kithiia, J., Cinner, J., Neale, E., Noble, S., Charles, D., and Watson, J.E. (2016). Integrating social–ecological vulnerability assessments with climate forecasts to improve local climate adaptation planning for coral reef fisheries in Papua New Guinea. Reg. Environ. Change *16*, 881–891. https://doi.org/10.1007/s10113-015-0807-0.

62. Melbourne-Thomas, J., Audzijonyte, A., Brasier, M.J., Cresswell, K.A., Fogarty, H.E., Haward, M., Hobday, A.J., Hunt, H.L., Ling, S.D., McCormack, P.C., et al. (2022). Poleward bound: adapting to climate-driven species redistribution. Rev. Fish Biol. Fish. *32*, 231–251. https://doi.org/10.1007/s11160-021-09641-3.

63. Lowerre-Barbieri, S.K., Catalán, I.A., Frugård Opdal, A., and Jørgensen, C. (2019). Preparing for the future: integrating spatial ecology into ecosystem-based management. ICES J. Mar. Sci. *76*, 467–476. https://doi.org/10.1093/icesjms/fsy209.

64. Zhou, S., Williams, A.P., Berg, A.M., Cook, B.I., Zhang, Y., Hagemann, S., Lorenz, R., Seneviratne, S.I., and Gentine, P. (2019). Land–atmosphere feedbacks exacerbate concurrent soil drought and atmospheric aridity. Proc. Natl. Acad. Sci. USA *116*, 18848–18853. https://doi.org/10.1073/pnas.1904955116.

65. Ciais, P., Reichstein, M., Viovy, N., Granier, A., Ogée, J., Allard, V., Aubinet, M., Buchmann, N., Bernhofer, C., Carrara, A., et al. (2005). Europe-wide reduction in primary productivity caused by the heat and drought in 2003. Nature *437*, 529–533. https://doi.org/10.1038/nature03972.

66. Xu, M., Zhang, T., Zhang, Y., Chen, N., Zhu, J., He, Y., Zhao, T., and Yu, G. (2021). Drought limits alpine meadow productivity in northern Tibet. Agric. For. Meteorol. *303*, 108371. https://doi.org/10.1016/j.agrformet.2021.108371.

67. Zhang, T., Zheng, X., Wang, X., Zhao, H., Wang, T., Zhang, H., Li, W., Shen, H., Yu, L., and Yu, G. (2018). Water availability is more important than temperature in driving the

carbon fluxes of an alpine meadow on the Tibetan Plateau. Int. J. Mol. Sci. *19–257*, 22–31. https://doi.org/10.1016/j.agrformet.2018.02.027.

68. Jolly, W.M., Cochrane, M.A., Freeborn, P.H., Holden, Z.A., Brown, T.J., Williamson, G.J., and Bowman, D. (2015). Climate-induced variations in global wildfire danger from 1979 to 2013. Nat. Commun. *6*, 7537. https://doi.org/10.1038/ncomms8537.

69. Dale, V.H., Joyce, L.A., Mcnulty, S., Neilson, R.P., Ayres, M.P., Flannigan, M.D., Hanson, P.J., Irland, L.C., Lugo, A.E., Peterson, C.J., et al. (2001). Climate change and forest disturbances. Bioscience *51*, 723. https://doi.org/10.1641/0006-3568(2001)051[0723:CCAFD]2.0.CO;2.

70. Gonzalez, P., Neilson, R.P., Lenihan, J.M., and Drapek, R.J. (2010). Global patterns in the vulnerability of ecosystems to vegetation shifts due to climate change. Global Ecol. Biogeogr. *19*, 755–768. https://doi.org/10.1111/j.1466-8238.2010.00558.x.

71. Gauthier, S., Bernier, P., Burton, P.J., Edwards, J., Isaac, K., Isabel, N., Jayen, K., Le Goff, H., and Nelson, E.A. (2014). Climate change vulnerability and adaptation in the managed Canadian boreal forest. Environ. Rev. *22*, 256–285. https://doi.org/10.1139/er-2013-0064.

72. Fonseca, M.G., Alves, L.M., Aguiar, A.P.D., Arai, E., Anderson, L.O., Rosan, T.M., Shimabukuro, Y.E., and de Aragão, L. (2019). Effects of climate and land-use change scenarios on fire probability during the 21st century in the Brazilian Amazon. Global Change Biol. *25*, 2931–2946. https://doi.org/10.1111/gcb.14709.

73. Lunt, I.D., Byrne, M., Hellmann, J.J., Mitchell, N.J., Garnett, S.T., Hayward, M.W., Martin, T.G., McDonald-Maddden, E., Williams, S.E., and Zander, K.K. (2013). Using assisted colonisation to conserve biodiversity and restore ecosystem function under climate change. Biol. Conserv. *157*, 172–177. https://doi.org/10.1016/j.biocon.2012.08.034.

74. Miller, C.H., Adame, B.J., and Moore, S.D. (2013). A review of recent advances in risk analysis for wildfire management. Disasters *37*, 1–27. https://doi.org/10.1071/WF11114.

75. Millar, C.I., Stephenson, N.L., and Stephens, S.L. (2007). Climate change and forests of the future: managing in the face of uncertainty. Ecol. Appl. *17*, 2145–2151. https://doi.org/10.1890/06-1715.1.

76. He, M., Piao, S., Huntingford, C., Xu, H., Wang, X., Bastos, A., Cui, J., and Gasser, T. (2022). Amplified warming from physiological responses to carbon dioxide reduces the potential of vegetation for climate change mitigation. Commun. Earth Environ. *3*, 160. https://doi.org/10.1038/s43247-022-00489-4.

77. Szeicz, J.M., and MacDonald, G.M. (1994). Age-dependent tree-ring growth responses of subarctic white spruce to climate. Can. J. For. Res. *24*, 120–132. https://doi.org/10.1139/x94-017.

78. Cao, S., Sun, G., Zhang, Z., Chen, L., Feng, Q., Fu, B., McNulty, S., Shankman, D., Tang, J., Wang, Y., and Wei, X. (2011). Greening China naturally. Ambio *40*, 828–831. https://doi.org/10.1007/s13280-011-0150-8.

79. Miyawaki, A. (2004). Restoration of living environment based on vegetation ecology: theory and practice: restoration of living environment. Ecol. Res. *19*, 83–90. https://doi.org/10.1111/j.1440-1703.2003.00606.x.

80. Hersbach, H., Bell, B., Berrisford, P., Hirahara, S., Horányi, A., Muñoz-Sabater, J., Nicolas, J., Peubey, C., Radu, R., Schepers, D., et al. (2020). The ERA5 global reanalysis. Q. J. R. Meteorol. Soc. *146*, 1999–2049. https://doi.org/10.1002/qj.3803.

81. Eyring, V., Bony, S., Meehl, G.A., Senior, C.A., Stevens, B., Stouffer, R.J., and Taylor, K.E. (2016). Overview of the coupled model Intercomparison Project phase 6 (CMIP6) experimental design and organization. Geosci. Model Dev. (GMD) *9*, 1937–1958. https://doi.org/10.5194/gmd-9-1937-2016.

82. Pu, J., Yang, J., Lu, S., Jin, D., Lai, X.H., Zhang, G., Tian, Z., Li, J., Wu, X., Huang, Y., et al. (2019). Evaluation of FAMIL2 in simulating the climatology and seasonal-to-interannual variability of tropical cyclone characteristics. Int. J. Syst. Evol. Microbiol. *69*, 1117–1122. https://doi.org/10.1029/2018MS001506.

83. Zhou, L., Bao, Q., Liu, Y., Wu, G., Wang, W.-C., Wang, X., He, B., Yu, H., and Li, J. (2015). Global energy and water balance: characteristics from finite-volume atmospheric model of the IAP/LASG (FAMIL1). J. Adv. Model. Earth Syst. *7*, 1–20. https://doi.org/10.1002/2014MS000349.

84. Liu, H., Lin, P., Yu, Y., and Zhang, X. (2012). The baseline evaluation of LASG/IAP climate system ocean model (LICOM) version 2. Acta Meteorol. Sin. *26*, 318–329. https://doi.org/10.1007/s13351-012-0305-y.

85. Lawrence, D.M., Oleson, K.W., Flanner, M.G., Thornton, P.E., Swenson, S.C., Lawrence, P.J., Zeng, X., Yang, Z.-L., Levis, S., Sakaguchi, K., et al. (2011). Parameterization improvements and functional and structural advances in version 4 of the community land model: parameterization improvements and functional and structural advances. J. Adv. Model. Earth Syst. *3*, M03001. https://doi.org/10.1029/2011MS00045.

86. Tebaldi, C., Debeire, K., Eyring, V., Fischer, E., Fyfe, J., Friedlingstein, P., Knutti, R., Lowe, J., O'Neill, B., Sanderson, B., et al. (2021). Climate model projections from the scenario model Intercomparison Project (ScenarioMIP) of CMIP6. Earth Syst. Dyn. *12*, 253–293. https://doi.org/10.5194/esd-12-253-2021.

87. O'Neill, B.C., Tebaldi, C., van Vuuren, D.P., Eyring, V., Friedlingstein, P., Hurtt, G., Knutti, R., Kriegler, E., Lamarque, J.-F., Lowe, J., et al. (2016). The scenario model Intercomparison Project (ScenarioMIP) for CMIP6. Geosci. Model Dev *9*, 3461–3482. https://doi.org/10.5194/gmd-9-3461-2016.

88. Holben, B.N. (1986). Characteristics of maximum-value composite images from temporal AVHRR data. Int. J. Rem. Sens. *7*, 1417–1434. https://doi.org/10.1080/01431168608948945.

89. Carlson, T.N., and Ripley, D.A. (1997). On the relation between NDVI, fractional vegetation cover, and leaf area index. Remote Sens. Environ. *62*, 241–252. https://doi.org/10.1016/S0034-4257(97)00104-1.

90. McArdle, B.H. (1988). The structural relationship: regression in biology. Can. J. Zool. *66*, 2329–2339. https://doi.org/10.1139/z88-348.

91. Shapiro, S.S., and Wilk, M.B. (1965). An analysis of variance test for normality (complete samples). Biometrika *52*, 591–611. https://doi.org/10.1093/biomet/52.3-4.591.

92. Liaw, A., and Wiener, M. (2002). Classification and regression by randomForest. R. News *23*.

93. Breiman, L. (2001). Random forests. Mach. Learn. *45*, 5–32. https://doi.org/10.1023/A:1010933404324.

94. van Beijma, S., Comber, A., and Lamb, A. (2014). Random forest classification of salt marsh vegetation habitats using quad-polarimetric airborne SAR, elevation and optical RS data. Remote Sens. Environ. *149*, 118–129. https://doi.org/10.1016/j.rse.2014.04.010.

95. Cutler, D.R., Edwards, T.C., Beard, K.H., Cutler, A., Hess, K.T., Gibson, J., and Lawler, J.J. (2007). Random forests for classification in ecology. Ecology *88*, 2783–2792. https://doi.org/10.1890/07-0539.1.

96. L. Breiman, ed. (1984). Classification and regression trees (Wadsworth International Group).

97. Congalton, R.G. (1991). A review of assessing the accuracy of classifications of remotely sensed data. Remote Sens. Environ. *37*, 35–46. https://doi.org/10.1016/0034-4257(91)90048-B.

STAR★METHODS

KEY RESOURCES TABLE

REAGENT or RESOURCE	SOURCE	IDENTIFIER
Deposited data		
Global meteorological reanalysis data (ERA5-Land)	European Centre for Mesoscale Weather Forecasts	https://cds.climate.copernicus.eu/cdsapp#!/dataset/reanalysis-era5-land-monthly-means
MODIS Vegetation Indices data (MOD13C2)	National Aeronautics and Space Administration	https://ladsweb.modaps.eosdis.nasa.gov/search/order/1/MOD13C2–6
Terra Advanced Spaceborne Thermal Emission and Reflection Radiometer Global Digital Elevation Model data	National Aeronautics and Space Administration	https://lpdaac.usgs.gov/products/astgtmv003/
MODIS Land Use/Cover Change data (MCD12Q1)	National Aeronautics and Space Administration	https://ladsweb.modaps.eosdis.nasa.gov/search/order/1/MCD12Q1–6
Global climate projection in CMIP6 simulations (FGOALS-f3)	Chinese Academy of Sciences	https://esgf-node.llnl.gov/projects/cmip6/
Software and algorithms		
ArcGIS	ESRI	https://www.arcgis.com/index.html
MATLAB 2018a	Mathworks	https://www.mathworks.com/products/matlab.html
Origin 2022b	OriginLab	https://www.originlab.com/OriginProLearning.aspx
MRT	National Aeronautics and Space Administration	https://lpdaac.usgs.gov/tools/modis_reprojection_tool/

RESOURCE AVAILABILITY

Lead contact

Further information for data and code files should be directed to and will be fulfilled by the lead contact, Xueqin Zhang (zhangxq@igsnrr.ac.cn).

Materials availability

This study did not generate new unique reagents.

Data and code availability

DATA: All datasets used in this study are publicly available: MODIS EVI (MOD13C2), land cover (MCD12Q1), and DEM (ASTER GDEM V3) data used in this study were obtained from the National Aeronautics and Space Administration (MOD13C2: https://ladsweb.modaps.eosdis.nasa.gov/search/order/1/MOD13C2–6, MCD12Q1: https://ladsweb.modaps.eosdis.nasa.gov/search/order/1/MCD12Q1–6; ASTER GDEM V3: https://lpdaac.usgs.gov/products/astgtmv003/). The meteorological data used in this study included the ERA5-Land reanalysis data provided by European Centre for Mesoscale Weather Forecasts (ECMWF) (https://cds.climate.copernicus.eu/cdsapp#!/dataset/reanalysis-era5-land-monthly-means) and the CMIP 6 climate projection data developed by Chinese Academy of Sciences (https://esgf-node.llnl.gov/projects/cmip6/).

CODE: This paper does not report original code.

Any additional information required to reanalyze the data reported in this paper is available from the lead contact upon request.

METHOD DETAILS

Climatic and environmental data

The climate and environmental data mainly include ERA5 (ECMWF's Reanalysis 5) and MODIS (The Moderate Resolution Imaging Spectroradiometer) data in this research. ERA5 data is produced by ECMWF (https://cds.climate.copernicus.eu), providing records of the global land surface with a horizontal resolution of 0.1°×0.1° since the 1980s.[80] Here we adopted the monthly averages of temperature, precipitation, wind speed, air pressure, evaporation, and potential evaporation from 2000 to 2021.

MODIS data also describes the features of the land surface on a global scale (https://ladsweb.modaps.eosdis.nasa.gov/). Therefore, we used the MODIS Vegetation Indices data (MOD13C2), a set of vegetation index data that provides NDVI (Normalized Differential Vegetation Index), EVI (Enhanced Vegetation Index), VIQA (Vegetation Index Quality Assessment), and reflectance data with a spatial resolution of 0.05 degree CMG (Climate Modeling Grid) (https://modis.gsfc.nasa.gov/data/). We adopted EVI data to calculate the fractional vegetation coverage (FVC).

Furthermore, we used the Terra Advanced Spaceborne Thermal Emission and Reflection Radiometer (ASTER) Global Digital Elevation Model (GDEM) data (ASTER GDEM V3, https://lpdaac.usgs.gov/products/astgtmv003/) and the MODIS LUCC (Land Use/Cover Change) (MCD12Q1) to describe the global elevation and land cover change, respectively. In addition, we resampled the vegetation and LUCC data based on bilinear (for EVI data and GDEM) and the nearest neighbor (for LUCC) interpolations to the same resolution (0.1°×0.1°) as ERA5 data, ensuring the consistency of multi-source data resolution.

CMIP6 simulations

The Coupled Model Intercomparison Project (CMIP) has become the foundational element of modern climate science and is now in its sixth phase (CMIP6).[81] We here used the future (2021 to 2080) temperature, precipitation, wind speed, air pressure, and evaporation data from the CMIP6 simulations produced by the CAS FGOALS-f3 (Chinese Academy of Sciences Flexible Global Ocean-Atmosphere-Land System Finite-Volume version 3) (https://esgf-node.llnl.gov/projects/cmip6/), the latest version of the Chinese Academy of Sciences climate system model designed for CMIP6. This model mainly includes the atmospheric component (Finite-volume Atmospheric Model version 2, FAMIL2),[82,83] oceanic component (LASG-IAP Climate System Ocean Model version 3, LICOM3),[84] land surface component (Community Land Model version 4.0, CLM4),[85] and sea ice component (Los Alamos Sea Ice Model version 4.0, CICE 4.0) (http://oceans11.lanl.gov/trac/CICE). Besides, the Community Earth System Model (CESM) is also introduced to couple these four components. Here, we adopted the low-resolution (about 100 km) FGOALS-f3 model (FGOALS-f3-L) to predict the future global CRTP distribution.

Meanwhile, CMIP6 data proposes a shared socioeconomic pathways (SSPs) framework describing future society's five alternative evolutions (SSP 1 to 5).[86] Combined with four representative concentration pathways (RCPs) in CMIP5, CMIP6 develops radiative forcing pathways. We selected four representative pathways: SSP 1–2.6, SSP 2–4.5, SSP 3–7.0, and SSP 5–8.5, corresponding to RCP 2.6, RCP 4.5, RCP 7.0, and RCP 8.5, respectively. The radiative forcing increases from SSP 1–2.6 to SSP 5–8.5. SSP 1–2.6 represents the low forcing sustainability pathway with a radiative forcing of 2.6 W m^{-2}, while SSP 5–8.5 represents the high radiative forcing scenario (8.5 W m^{-2}).[87]

FVC calculation

The maximum value composite (MVC) method and a filter based on the land cover types and the continuity were utilized to control the quality of remote sensing data and extract the annual maximum EVI value at each pixel.[39,88] Then, based on the maximum EVI, we calculated FVC, the proportion of the vertical projection of vegetation to the total area, to describe the regional vegetation coverage. FVC in the limited region can be calculated with the following Equation[89]:

$$FVC = \frac{EVI - EVI_{soil}}{EVI_{veg} - EVI_{soil}} \quad \text{(Equation 1)}$$

Where EVI_{soil} and EVI_{veg} represent the EVI value in bare soil and pure vegetation areas, respectively. For the multi-year global data, here we replaced the EVI_{soil} and EVI_{veg} with the value in the theoretical ideal state (0 and 1) to ensure the applicability to various conditions.

Trend of vegetation and climate change

We used linear regression based on the ordinary least square method (OLS) to calculate the trend of the climate and vegetation. The sequence of temperature, precipitation, or FVC in each grid from 2000 to 2021 is considered independent sequence samples. OLS is adopted to seek the best-fitting result by minimizing the sum of squared errors.[90] Additionally, we adopted the F-test method to test the statistical significance of the regression regarding the slope of the fitting straight line as the trend of FVC or climatic factors.

CRTP calculation and classification

We proposed an innovative index CRTP to quantitatively compare the impacts of temperature and precipitation on vegetation change. We first selected a group of climatic factors (temperature, precipitation, wind speed, air pressure, evaporation, and potential evaporation). Then we introduced the Analysis of Variance (ANOVA) method[91] to quantify the relative contribution of each climatic factor to vegetation change. The CRTP value is the logarithm of the ratio of the relative contribution of temperature (R_{temp}) and precipitation (R_{prep}):

$$CRTP = \log_{10}\left(\frac{R_{temp}}{R_{prep}}\right) \quad \text{(Equation 2)}$$

Since the relative contribution of temperature and precipitation to vegetation change (R_{temp}) and precipitation (R_{prep}) is equal to the ratio of the sum of square deviations (SS) to the total sum of square (SST), CRTP can be simplified as follow:

$$CRTP = \log_{10}\left(\frac{SS_{temp}/SST}{SS_{prep}/SST}\right) = \log_{10}\left(\frac{SS_{temp}}{SS_{prep}}\right) \quad \text{(Equation 3)}$$

where SS_{temp} and SS_{prep} represent the sum of square deviations of temperature and precipitation, respectively. CRTP in different thresholds corresponds to various vegetation change mechanisms. Hence, we classified global vegetation change into four types according to the CRTP value: Type 1 (CRTP less than −1, precipitation dominates FVC change), Type 2 (CRTP from −1 to 0, FVC is mainly affected by precipitation and supplemented by temperature), Type 3 (CRTP from 0 to 1, FVC is primarily influenced by temperature and supplemented by precipitation), and Type 4 (CRTP greater than 1, temperature dominates FVC change). Precipitation tends to predominate the vegetation change in regions with CRTP negative (Type 1 and 2). Similarly, the temperature is more likely to dominate vegetation coverage in areas with CRTP positive (Type 3 and 4). Besides, the CRTP value greater than 1 (or less than −1) indicates that the impact of temperature (precipitation) is more overwhelming than that of precipitation (temperature).

Noteworthy, we designed the index CRTP to simplify the complex relationship between vegetation and climate. To eliminate interference from non-climatic factors, such as human activities, we defined this index as statistically significant only for regions where climatic factors dominate the vegetation change.

Random forest optimal model for CRTP classification and prediction

The supremacy of temperature and precipitation on vegetation change is interchanged with regions, seasons, and species.[12,16] So, we can deduce that regional CRTP type highly depends on the local climatic, geographic, and environmental conditions. Assuming a stable and reliable relationship exists between CRTP and some constant (e.g., longitude, latitude, and altitude) or predictable factors (e.g., climatic factors), we could build the CRTP classification model based on these predictable factors. Then, we could predict the future CRTP type by predicting these climatic, geographic, or environmental factors.

Here, we utilized the RF ("randomForest" package in R[92]) classifier to construct the CRTP classification prediction models based on predictable climatic, geographic, and environmental factors. The RF algorithm depends on decision tree classification,[93] which has been extensively applied in climate and ecological research.[94,95] We fitted a predefined number of classification trees to a dataset (500 in this research) and combined the predictions from all trees, achieving an output determined by a majority vote among the decision trees.[96] Multiple data sets with different numbers and climatic and environmental data combinations were selected as the input variables. Each pixel with statistically significant CRTP was considered a single sample. Then, we used the "Caret" package in R to sample the data with 80% as the training set and the rest as the test set. The classification accuracy of the test set was considered the accuracy of each model. Here,

the overall accuracy, kappa coefficient, and error matrix were adopted for the accuracy assessment of RF classification.

We performed the overall accuracy and kappa coefficient on all classification results with different input variables and displayed the error matrix on the optimal classification model. As indicators to measure classification accuracy, the overall accuracy and kappa coefficient can be extracted from the error matrix.[97] The overall accuracy is the proportion of the number of correctly classified samples to the number of all samples. The kappa coefficient can be calculated as follows:

$$p_e = \frac{a_1 \times b_1 + a_2 \times b_2 + \ldots + a_c \times b_c}{n \times n} \quad \text{(Equation 4)}$$

$$Kappa = \frac{p_0 - p_e}{1 - p_e} \quad \text{(Equation 5)}$$

In these formulas, a_1, a_2, …, a_c, are the numbers of correctly classified samples of each category, while b_1, b_2, …, b_c, are the predicted samples of each category. *Kappa* represents the kappa coefficient, and p_0 is the overall accuracy. The value range of the kappa coefficient is usually [0, 1]. The larger this coefficient, the higher the classification accuracy.

Here, we built the CRTP classification model according to different climatic (temperature, precipitation, wind speed, air pressure, evaporation, and potential evaporation), geographic (longitude, latitude, altitude, and distance from sea), and environmental (FVC, LUCC) factors based on machine learning. Given the relative contributions of different climatic factors to vegetation change highly depending on the hydrothermal conditions and the magnitudes of climate change,[24,42] we extracted the climatic information of these two aspects to analyze its attribution to CRTP distribution. First, we calculated the annual average of climatic factors to describe the regional climatic condition and extracted the change rate using the OLS method. Then, different climatic factors' average values and change rates are input into the RF model as variables representing each independent climatic factor. Besides, we selected the average FVC from 2000 to 2021 and the land cover type in the middle of the period (2010 in this research) as the input variables to ensure that environmental variables can represent the environmental characteristics in a certain period. We also screened the global samples according to the land cover type before inputting them into the model. Samples corresponding to croplands and settlements are removed because CRTP and related models at the present stage only consider the natural processes.

We first input climatic variables with different combinations and obtained the temporary best model by comparing the accuracy to achieve the optimal set of input variables. Secondly, we gradually added geographic variables to form new models and got an optimal climatic-geographic model. Then, we added environmental variables and produced the final optimal model. Notably, multiple (usually five) simulations were repeatedly run on the same set of variables, screening the model with the highest accuracy. In particular, over ten simulations were repeated on two sets of variables with similar model accuracy to help precisely pick out the better model.